NEOPLASIA
www.neoplasia.com

Volume 12 Number 4 April 2010 pp. 317–325 317

Senescent Fibroblasts Promote Neoplastic Transformation of Partially Transformed Ovarian Epithelial Cells in a Three-dimensional Model of Early Stage Ovarian Cancer[1,2]

Kate Lawrenson*[,3], Barbara Grun*, Elizabeth Benjamin†, Ian J. Jacobs*, Dimitra Dafou* and Simon A. Gayther*

*Gynaecological Cancer Research Laboratories, UCL EGA Institute for Women's Health, University College London, London, UK; †Department of Histopathology, Royal Free/UCL Medical School, Rockefeller Building, London, UK

Abstract

Most epithelial ovarian cancers are diagnosed postmenopausally, although the well-established epidemiological risk factors (parity, oral contraceptive use) are premenopausal. We hypothesized that accumulation of senescent fibroblasts, together with concomitant loss of presenescent fibroblasts within the ovarian cortex, promotes initiation and early development of ovarian cancer from ovarian surface epithelial (OSE) cells. To test this, we established immortalized OSE (IOSE) cell lines that mimic early neoplastic transformation by overexpressing the *CMYC* oncogene ($IOSE^{CMYC}$) and normal ovarian presenescent (PSN) and senescent (SEN) fibroblast cell lines. We then evaluated the ability of PSN and SEN fibroblasts to transform IOSE and $IOSE^{CMYC}$ after coculture. SEN fibroblasts significantly enhanced neoplastic development of $IOSE^{CMYC}$ cells; there was an up to 15-fold increase in migration of $IOSE^{CMYC}$ cells cocultured with SEN fibroblasts compared with PSN fibroblasts. Conditioned medium from SEN fibroblasts promoted anchorage-independent growth of $IOSE^{CMYC}$ cells. We studied fibroblast-epithelial cell interactions in heterotypic three-dimensional spheroid models. Dual immunohistochemical staining of spheroids for a proliferation marker (MIB-1) and cytokeratin-18 indicated that SEN fibroblasts induce approximately a five-fold increase in proliferation of $IOSE^{CMYC}$ cells relative to cocultures with PSN fibroblasts. SEN, but not PSN fibroblasts, also induced nuclear atypia in epithelial cells in three-dimensional spheroids. These data suggest for the first time that the accumulation of senescent, or loss of presenescent fibroblasts, can promote neoplastic development of partially transformed OSE cells *in vitro* and illustrates the power of using three-dimensional heterotypic modeling to gain better insights into the etiology underlying the development of epithelial ovarian cancer.

Neoplasia (2010) 12, 317–325

Introduction

More than 80% of all epithelial ovarian cancers (EOCs) are diagnosed in postmenopausal women older than 60 years [1,2]. However, the strongest epidemiological risk factors for EOC are premenopausal factors (oral contraceptive pill use and parity) [3,4]. High-grade serous tumors are the most common histopathologic subtype of the disease but are rarely diagnosed at an early stage, suggesting that these tumors progress rapidly. One hypothesis to explain postmenopausal disease development is that some as yet unknown microenvironmental trigger initiates proliferation in dormant epithelial cells that harbor somatic mutation(s). One possible trigger could be age-related changes (senescence) occurring in ovarian stromal fibroblasts, which work in synergy with early genetic changes in the epithelium to promote EOC development.

Abbreviations: NOF, normal ovarian fibroblast; INOF, immortalized NOF; SEN, senescent NOF; PSN, presenescent NOF; OSE, ovarian surface epithelium; IOSE, immortalized ovarian surface epithelium

Address all correspondence to: Kate Lawrenson, PhD, MRC Laboratory for Molecular Cell Biology, University College London, Gower Street, London, WC1E 6BT, UK.
E-mail: kate.lawrenson@ucl.ac.uk

[1]This work was funded by Medical Research Council studentships (K.L. and B.G.), the Eve Appeal Gynaecology Cancer Research Fund, the Rosetrees Trust, and by a charitable donation from UCLH special trustees.

[2]This article refers to supplementary material, which is designated by Figure W1 and is available online at www.neoplasia.com.

[3]Current address: MRC Laboratory for Molecular Cell Biology, University College London, Gower Street, London, WC1E 6BT, UK.

Received 23 November 2009; Revised 26 January 2010; Accepted 27 January 2010

DOI 10.1593/neo.91948

As an organism ages, senescent fibroblasts accumulate in the tissue stroma, gradually replacing presenescent cells [5,6]. *In vitro* and *in vivo* models have demonstrated that normal fibroblasts in a normal tissue microenvironment can inhibit early tumorigenesis but that fibroblast senescence results in a loss of inhibition of tumorigenesis and/or promotion of epithelial transformation [7–9]. For example, senescent fibroblasts enhance epithelial neoplastic progression *in vitro* and promote the formation of tumor xenografts *in vivo* in models of mammary, prostate, and keratinocyte tumors [10–13]. Senescent cells do not divide but remain metabolically active, and the profile of secreted proteins in senescent cells differs substantially from their nonsenescent counterparts [14]. The induction of senescence induces a senescence-associated secretory phenotype; senescent fibroblasts secrete a multitude of growth factors (including vascular endothelial growth factor), extracellular matrix proteins, proteases, chemokines, and cytokines [14,15]. It is likely that these molecules act in paracrine to affect the phenotype of neighboring epithelium, directly and indirectly, through remodeling of the extracellular matrix and/or through interaction with other cell types (e.g., inflammatory or endothelial cells) [8,16].

The aim of the current study was to investigate the role of aging fibroblasts in the initiation and development of EOCs, using a three dimensional model of cellular transformation of the ovarian surface epithelium (OSE). We have previously established three-dimensional cell culture models of normal, primary OSE cells and demonstrated their biological similarities to primary tissues [17]. In the current study, we created a three-dimensional heterotypic model of ovarian stromal-epithelial cell interactions, and of the earliest stages of OSE transformation, to test the hypothesis that accumulation of senescent fibroblasts, with concomitant loss of presenescent stromal cells, contributes to transformation of ovarian epithelial cells. The results imply a role for senescent fibroblasts in promoting early tumorigenesis of OSE and further suggest that the ovarian stromal microenvironment may have a crucial role in the development of EOCs.

Materials and Methods

Cell Culture, Retroviral Production, and Transduction

Primary normal ovarian surface epithelial (NOSE) cell isolates NOSE4, NOSE11, and NOSE19L3 have been previously described [17]. All ovarian epithelial cell cultures were maintained in NOSE medium (NOSE-CM) [17]. Normal ovarian fibroblast (NOF) cells were isolated from a patient undergoing total abdominal hysterectomy for endometrial carcinoma. The ovary was confirmed as free of disease by a gynecological pathologist (E.B.). A tissue sample was excised from the ovary and washed twice with phosphate-buffered saline (PBS; from VWR, Lutterworth, UK) to remove loosely attached epithelial cells. Tissue was then minced and incubated at 37°C/5% CO_2 for 7 to 14 days to allow colony growth. Colonies with fibroblastic morphologies were isolated. Fibroblast cultures were maintained in basic medium MCDB105/Medium 199 (1:1 ratio; both Sigma, St Louis, MO), 15% fetal bovine serum (FBS), and 1% L-glutamine (both Invitrogen, Paisley, UK). To induce senescence, cells were exposed for 2 hours to 80 μM of hydrogen peroxide solutions (VWR) diluted in culture medium. β-Galactosidase bioactivity assays were performed as previously described [18]. Senescent fibroblasts were freshly prepared for replicate experiments.

293T cells at 70% confluence were cotransfected with the pVPack10A1, pVPackGP, and pBabe.hygro.hTERT/ pWZL.Blast. CMYC (Addgene) vectors using FuGene6 transfection reagent (Roche, Basel, Switzerland) at ratio of 3:1, reagent/DNA. The medium was replaced 16 hours after transfection, and cultures were incubated for a further 48 hours before retroviral supernatants were harvested and stored at −80°C. To infect recipient cells, 3 ml of supernatant and 4 μg/ml DEAE-dextran (Sigma) were added to NOSE/NOF cells at 30% to 50% confluence. Cells were split the following day, and positive cells were selected with 10 to 30 U/ml hygromycin B (Merck, Darmstadt, Germany)/2 to 3 μg/ml blasticidin (Sigma).

Immunofluorescent Cytochemistry and Immunohistochemistry

Immunofluorescent cytochemistry was performed using standard protocols. The following antibodies were used at 1:1000 dilutions: AE1/AE3 (Dako Corporation, Carpinteria, CA), cytokeratin 7 (CR-UK, London, UK), BerEp4 (Dako), CA-125 (Dako), E-cadherin (Cell Signaling, Danvers, MA), and fibroblast surface protein (FSP; Sigma). Alexa Fluor 488–coupled secondary antimouse or antigoat antibodies (Invitrogen) were used for antigen detection. Cells were counterstained with Evans Blue (Sigma) diluted in H_2O. Immunohistochemistry of three-dimensional cultures was performed using standard protocols at the UCL Advanced Diagnostics Laboratory. For analysis of MIB-1 and cytokeratin 18 (Ck18) dual staining, the proportion of MIB-1^+/$Ck18^+$ cells were calculated relative to the total $Ck18^+$ population of the culture, using the following formula: relative % dual positive cells = (number of MIB-1^+/$Ck18^+$ cells)/(total number of $Ck18^+$ cells)] × 100%.

Telomere Length and Telomerase Activity Assays, In Vitro *Analysis of Tranduced Clones*

To detect telomere length and telomerase activity, the Telo*TAGGG* Telomere Length Assay and Telomerase PCR ELISA^{PLUS} from Roche were used according to the manufacturer's protocols. For calculation of relative telomerase activity, an *hTERT*-immortalized fibroblast cell line (1BR3) was included as a positive control. Population doubling rates were measured for 1×10^5 cells, in triplicate. Cultures were passaged, and population doublings (PD) were calculated using the following formula: PD = log (total cell number at each passage/initial cell number)/$\log_2$. Anchorage-independent growth assays were performed as previously described [17]. Anchorage-dependent growth was assayed by plating 100 cells in six replicates onto 100-mm plates. Cells were refed three times a week for 2 weeks and then fixed with methanol and stained with Coomassie blue (Sigma). Colonies containing more than 10 cells were counted, and colony formation efficiencies were calculated using the following formula: colony-forming efficiency (CFE) = [(number of colonies counted)/(number of cells plated)] × 100%.

Real-time Polymerase Chain Reaction

RNA extractions were performed using the QIAgen RNA extraction kit with on-column DNase treatment. Samples were quantified and reverse-transcribed using random hexamer primers, according to standard protocols. For real-time polymerase chain reaction (PCR), samples were run according to manufacturer's protocols: a FAM-labeled real-time probe for *CMYC* (HS00153349_m1; Applied Biosystems, Carlsbad, CA) was used with 18S rRNA probe as an internal control. Samples were analyzed on an ABI 7900HT Fast Real-time PCR System (Applied Biosystems) and analyzed using the $\Delta\Delta C_t$ relative quantification method.

Flow Cytometry

Cell cultures were trypsinized and centrifuged, and cell pellets were resuspended in FACS buffer, with or without an anti–Annexin-FITC–labeled antibody, according to the manufacturer's instructions (Roche).

Samples were run on a Becton Dickinson FACS Scan (Franklin Lakes, NJ), and the Annexin V–positive population was measured. For cell cycle analysis, cells were incubated with 1 mM 5-bromo-2-deoxyuridine (BrdU; Sigma) for 2 hours. Cells were then washed in PBS and fixed by dropwise addition of 70% ethanol with constant agitation. Samples were incubated at 4°C overnight before extraction of nuclei using standard pepsin digestion protocols. Pelleted nuclei were incubated with an anti-BrdU antibody (Becton Dickinson), washed twice with IFA (10 mM HEPES pH 7.4, 150 mM NaCl, 0.1% sodium azide [all Sigma]; 4% FBS [Lonza, Basel, Switzerland]) and then incubated with an Alexa Fluor 488–coupled secondary antibody (Invitrogen). Washed nuclei were resuspended 100 μg/ml propidium iodide (Sigma) in PBS and analyzed as above.

Heterotypic Assays (Invasion, Migration, and Three-dimensional Cell Culture)

Standard invasion and migration assays were modified to use presenescent and senescent ovarian fibroblasts as a chemoattractant. A total of 9×10^4 fibroblasts were plated in 24-well plates. The following day, the cells were washed twice with PBS, and then 500 μl of serum-free medium was added. Migration chambers (Greiner, Frickenhausen, Germany) or rehydrated invasion chambers (Millipore, Billerica, MA) were placed atop the fibroblast monolayers, and 3×10^4 (for migration assays) and 12.5×10^4 (for invasion assays) epithelial cells were plated within the chamber. Assays were incubated at 37°C/5% CO_2 for 24 hours before detection of invaded/migrated cells. For invasion assays, invaded cells were detached from the membrane and lysed, and a quantitative fluorimetric dye was added, using reagents from the 24-well Chemicon QCM ECMatrix fluorimetric Invasion Assay Kit (Millipore). Relative fluorescence units were read on a Varioskan Flash plate reader (Thermo Scientific, Waltham, MA), and average values of a negative control (no cells) were deduced from each test well. For migration assays, migrated cells were quantified as above, or membranes were stained *in situ* with 1% crystal violet (Sigma) in 100% methanol, washed twice with distilled water, and air-dried. The migrated cells were counted in 10 fields of view per membrane. In all experiments, 10% FBS as a chemoattractant was also plated as a positive control.

Cells were grown as three-dimensional multicellular spheroids on plastic dishes coated twice with a 1.5% solution of poly-2-hydroxyethyl methacrylate (polyHEMA) from Sigma, prepared in 95% ethanol (also Sigma). Fibroblasts were plated onto polyHEMA-coated plates and allowed to form spheroids for 7 days before the culture was inoculated with epithelial cells at a ratio of 4:1 fibroblasts-epithelial cells. Three-dimensional heterotypic cultures were maintained in basic medium for 2 weeks and fed twice weekly before multicellular aggregates were harvested, fixed in neutral-buffered formalin (VWR), processed into paraffin, and stained by standard immunohistochemical techniques (at the CR-UK Histology Service). For two-dimensional indirect coculture assays, epithelial cells were plated into 24-well plates, and fibroblasts were seeded into permeable tissue culture inserts (Greiner) at a ratio of 4:1 fibroblasts-epithelial cells. After 24 hours, the two cell types were cocultured and maintained for 14 days with twice-weekly refeeding. Epithelial cells were then fixed with methanol and stained with crystal violet (5 mg/ml in 2% ethanol), and cells lysed with 2% SDS/dH_2O. Absorbance was then read at 595 nm on a Varioskan Flash plate reader.

Statistical Analysis

Where indicated, 2-tailed paired Student's *t*-tests were performed.

Results

Normal Ovarian Fibroblasts Can Be Immortalized by the Ectopic Expression of hTERT

Primary NOFs have a limited proliferative capacity *in vitro*. To address this, we used ectopic overexpression of the catalytic subunit of human telomerase (*hTERT*) to extend the life span of primary NOF cells beyond 100 days without signs of replicative senescence (Figure 1*A*). *hTERT* infected NOFs expressed telomerase, whereas primary NOFs showed no telomerase activity, suggesting that NOFs had been immortalized (INOFs; Figure 1*B*). Neither NOFs nor INOFs showed any evidence of tumorigenic transformation, evaluated by anchorage-independent growth. INOFs maintain expression of vimentin and FSP and did not express the epithelial cell marker Ck7 (Figure 1*C*). There was no expression of smooth muscle actin (SMA) in primary NOFs, but SMA expression in INOFs indicated an activated phenotype, which is consistent with other studies that show fibroblasts from other organs become activated after *hTERT* immortalization (Figure 1*C*) [19,20]. INOFs also maintained p16 expression, suggesting that loss of this cell cycle checkpoint is not required for immortalization. Similar observations have been reported after immortalization of human mammary epithelial cells, embryonic lung fibroblasts, and ovarian surface epithelial (OSE) cells [21–25]. As part of this study, we also *hTERT*-immortalized OSE (IOSE) cells derived from three different, normal, primary OSE cultures (IOSE4, IOSE11, and IOSE19) using previously described methods [17,24]. We confirmed that the primary OSE and IOSE cells used in this study exhibit both epithelial and nonneoplastic characteristics (Figure W1).

CMYC *Overexpression Induces Neoplastic Transformation of IOSE Cells*

A complementary DNA encoding full-length *CMYC* was introduced into IOSE cells by retroviral transduction to induce the early stages of neoplastic transformation. *CMYC* messenger RNA expression levels were increased 80 to 500-fold in CMYC-infected IOSE cell lines ($IOSE4^{CMYC}$, $IOSE11^{CMYC}$, and $IOSE19^{CMYC}$). $IOSE^{CMYC}$ cells displayed altered cell morphology with cell size decreased, cell shape more cuboidal, and cells more classically epithelial than IOSE cells. $IOSE^{CMYC}$ cells were tightly packed into a monolayer in traditional two-dimensional cultures and lost the mesenchymal scattering phenotype that is characteristic of IOSE cells (Figure 2*A*). $IOSE^{CMYC}$ cells also showed increased CFEs in anchorage-dependent and anchorage-independent growth assays ($P \le .01$; Figure 2, *B* and *C*). *CMYC* messenger RNA levels correlated with anchorage-independent CFE (Pearson's coefficient test, $r^2 = 0.8$, $P = .0156$, $\alpha = 0.05$). Flow cytometry showed significant reductions in the percentage of apoptotic cells in $IOSE^{CMYC}$ cell lines compared with the IOSE cell lines ($P \le .05$; Figure 2*D*). A significantly greater proportion of $IOSE^{CMYC}$ cells was in G_2 phase of the cell cycle ($P \le .05$; Figure 2*E*). These characteristics are all consistent with the suggestion that $IOSE^{CMYC}$ cells had undergone neoplastic transformation, although neither IOSE nor $IOSE^{CMYC}$ cells expressed the ovarian cancer markers E-cadherin and CA-125, suggesting that $IOSE^{CMYC}$ cells were only partially transformed.

Senescent Fibroblasts Enhance the Neoplastic Phenotype of $IOSE^{CMYC}$ Cells

We induced senescence in INOF cells by exposing the cells to low dose levels of hydrogen peroxide (H_2O_2). H_2O_2 exposure reduced proliferation of INOFs by approximately 30% and induced senescence,

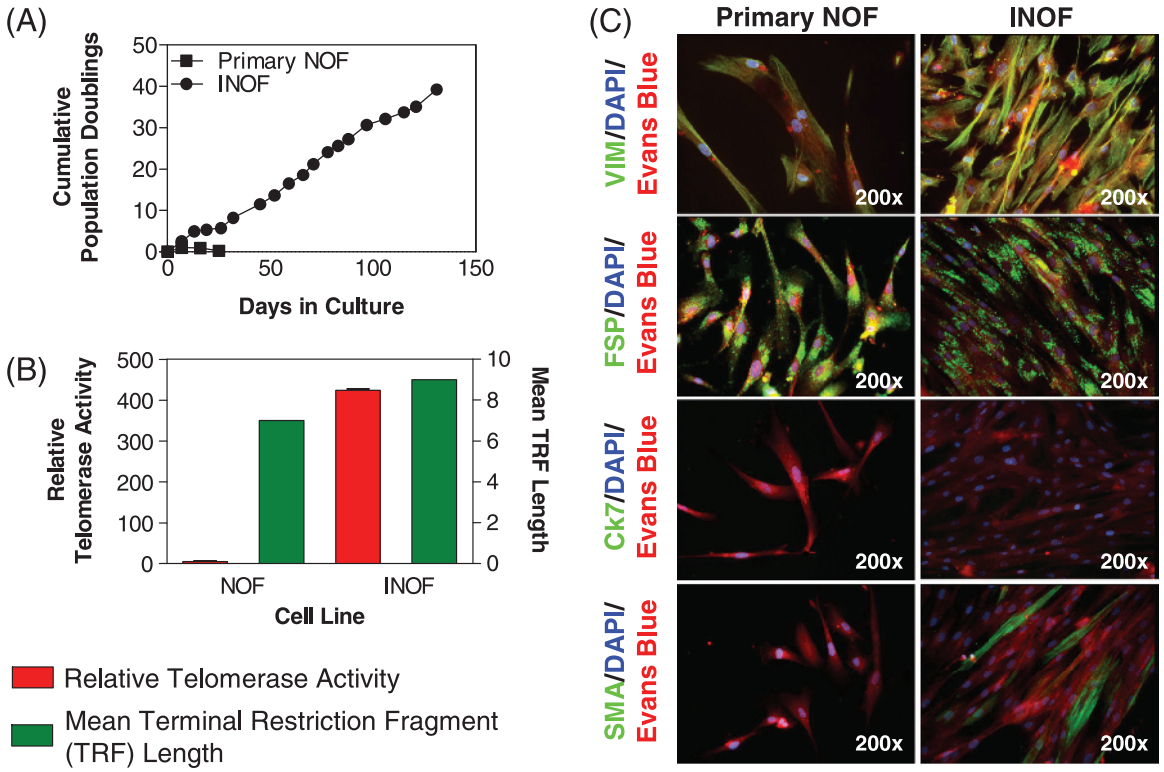

Figure 1. Extended life span of primary NOFs after *hTERT* immortalization. (A) Ectopic expression of *hTERT* increases the number of PDs of NOFs to more than 30 PDs in INOFs. (B) Telomerase activity (relative to an internal positive control) is negligible in cell extracts from primary NOFs but elevated in INOF cultures, and telomere terminal restriction fragment lengths are increased by approximately 2 kb after introduction of *hTERT*. (C) NOFs and INOFs both exhibit "spotty" positive staining with an anti-FSP antibody, which is characteristic of fibroblasts. Both cell lines stain negative for Ck7. SMA is expressed in approximately 30% of INOF cells indicating a transition toward an activated fibroblast phenotype with immortalization. Primary NOF cells did not express SMA, and this was independent of cell density. Both NOF and INOF cells express p16 in the nucleus and cytoplasm (arrows). 4′,6-Diamidino-2-phenylindole (blue) stains cell nuclei, Evan's blue (red) stains the cell cytoplasm, and green fluorescence denotes positive staining. Note the spindled morphology of fibroblast cells. Exposure times for immunofluorescent images were constant for each antigen. Error bars, SEM.

as shown by β-galactosidase expression (Figure 3*A*). We compared the effects of H_2O_2-treated senescent fibroblasts (SEN) and untreated presenescent fibroblasts (PSNs) on the invasive and migratory phenotypes of IOSE and IOSE^{CMYC} cells. There was a 5.7- to 7.2-fold reduction in transwell migration for all three IOSE^{CMYC} cell lines cocultured with PSN fibroblasts relative to a serum control ($P \leq .01$). In contrast, migration levels increased 3.8- to 14.9-fold compared with serum controls when IOSE^{CMYC} cells were cocultured with SEN fibroblasts (Figure 3*B*). SEN fibroblasts also increased the invasive ability of IOSE^{CMYC} cells compared with PSN fibroblasts ($P \leq .05$; Figure 3*C*). Neither PSN nor SEN fibroblasts had any significant effects on the invasive or migratory properties of IOSE cells. Finally, when we used conditioned medium (CM) from cultured SEN fibroblasts in anchorage-independent growth assays, we found that it increased the tumorigenic phenotype of IOSE19^{CMYC} cells relative to the same cells grown in CM from PSN fibroblasts ($P \leq .05$). Colony formation efficiencies of IOSE^{CMYC} cells grown in PSN-CM or SEN-CM were significantly reduced relative to cells grown in standard growth medium (NOSE-CM, $P \leq .05$; Figure 3*D*).

Senescent Fibroblasts Enhance Epithelial Proliferation in Three-dimensional Heterotypic Culture Models

Three-dimensional spheroid models of INOFs were generated by culturing cells on polyHEMA-coated tissue culture plastics. INOFs formed spontaneous aggregates within 48 hours of culture in nonadherent conditions. Examination of formalin-fixed, paraffin-embedded sections of 7-day-old INOF spheroids, stained with hematoxylin and eosin (H&E), revealed that the central regions of spheroids contain predominantly acellular hyalinized nodules with apoptotic cells distributed throughout a matrix-rich core. Peripherally, spindled cells with elongated nuclei and an eosinophilic cytoplasm surround the spheroid. PSN and SEN fibroblast spheroids were indistinguishable by H&E staining.

Seven-day-old INOF spheroid cultures were inoculated with IOSE cells (INOF/IOSE cells ratio of 4:1) to establish three-dimensional fibroblast-epithelial cell models. H&E examination of stained sections of these heterotypic three-dimensional cultures showed central hyalinized cores of abundant matrix protein (Figure 4, *A* and *B*). Spheroids consisted of two morphologically distinct populations of cells, with either spindled or plump cell morphologies. When IOSE cells were cultured with SEN fibroblasts, we observed nuclear atypia within populations of plump, peripheral cells and features such as irregular/enlarged nuclei, prominent nucleoli and "giant" mononuclear cells within peripheral regions of the spheroids (Figure 4*A*). These atypical features were not present in spheroids generated from IOSE cells cultured with PSN fibroblasts. There were also more prominent nucleoli and mitoses in the plump cell populations from SEN-IOSE^{CMYC} cocultures compared with PSN-IOSE^{CMYC} cocultures (Figure 4*B*). Finally, when IOSE^{CMYC} cells were cocultured with PSN fibroblasts, we saw marked apoptosis

in the central regions of spheroids, which was not present in SEN-IOSE^{CMYC} cocultures (data not shown).

IOSE/INOF spheroids were compared with normal ovarian tissues after staining for several epithelial and fibroblast markers. Only cytokeratin 18 (Ck18) reliably distinguished between ovarian fibroblasts and epithelial cells. The fibroblastic markers vimentin, desmin, and proline-4-hydroylase did not accurately discriminate between epithelial cells and fibroblasts in normal ovarian tissue samples and spheroid cultures (data not shown). In IOSE/INOF spheroids, epithelial cells could be identified by Ck18 staining; IOSE cells formed a single cell layer surrounding the fibroblast "core," reminiscent of the OSE monolayer *in vivo* (Figure 4*C*). However, in INOF-IOSE^{CMYC} cocultures, IOSE^{CMYC} cells formed multiple cell layers surrounding the fibroblast core, with some Ck18^{+} cells invading into the central regions of the spheroid (Figure 4, *E* and *F*). Dual immunohistochemical staining for Ck18 and the proliferation marker MIB-1 highlighted the actively proliferating epithelial proportion of culture (Figure 4, *C*–*F*). In three-dimensional cocultures, IOSE^{CMYC} cells were 0.03- to 12.8-fold more proliferative than IOSE cells. In SEN-IOSE^{CMYC} spheroids, there was a 1.4- to 4.7-fold increase in the relative percentage of IOSE^{CMYC} cell staining positive for both Ck18 and MIB-1 relative to PSN-IOSE^{CMYC} cocultures (Figure 4*G*). SEN/PSN fibroblasts did not significantly affect the proliferation of epithelial cells in two-dimensional cocultures (Figure 4*H*).

Discussion

The two most well-described risk factors for EOCs are the protective effects conferred by pregnancy and oral contraceptive use [3,4]. It has been postulated that both act by reducing the number of ovulations throughout a woman's lifetime, thus limiting the extent of rupture and repair of the OSE [26]. However, ovarian cancer usually occurs several years after menopause, and the natural history of high-grade serous tumors (the most common histopathologic subtype) suggests rapid and aggressive tumor growth. The microenvironmental trigger for this is unlikely to be hormonal factors, given that postmenopausal ovaries no longer produce mitogenic steroid hormones (neither estrogens nor androgens) [27]. Postmenopausal ovaries often show age-related histopathologic changes, such as increased numbers of inclusion cysts and deep invaginations of OSE into ovarian stroma, and it has been hypothesized that these may be associated with neoplastic transformation [28]. We hypothesized that loss of presenescent stromal fibroblasts and/or an accumulation of metabolically active but senescent fibroblasts

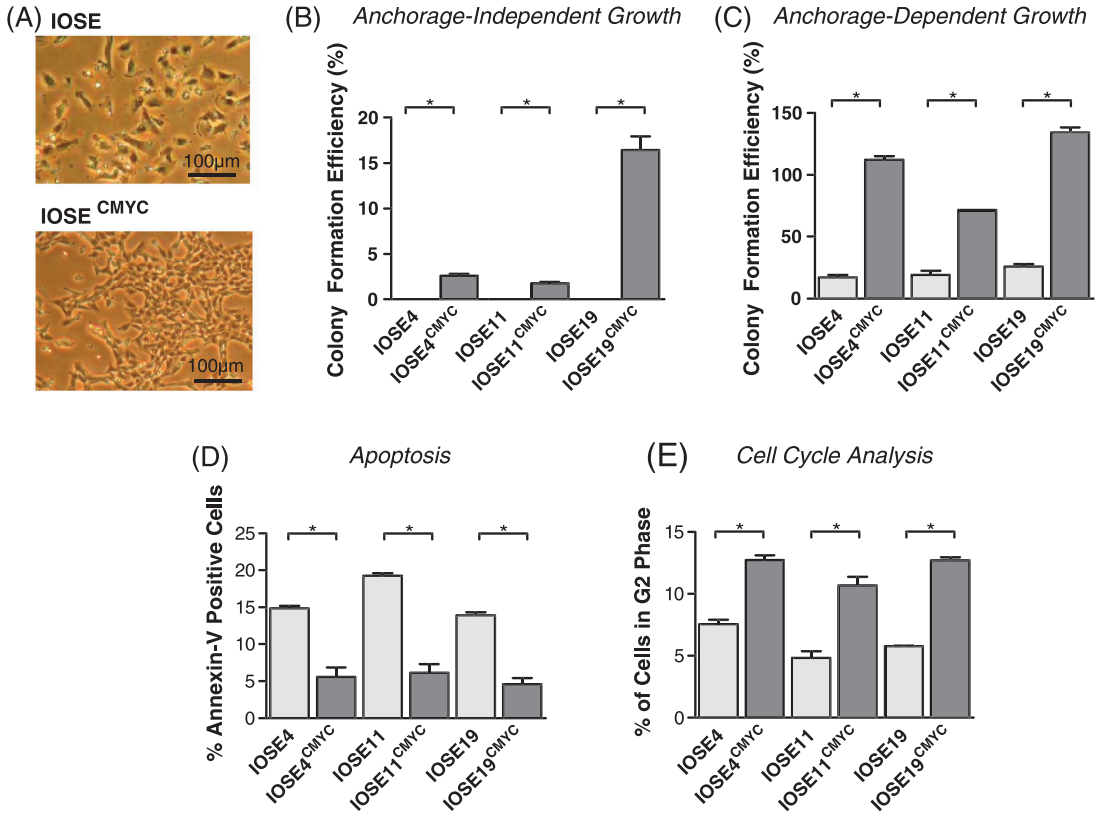

Figure 2. Immortalized OSE (IOSE) cell cultures overexpressing *CMYC* (IOSE^{CMYC} cells) show features of neoplastic transformation. (A) The fibroblast-like elongated morphology of IOSE cultures changes to a more typically epithelial (cuboidal) morphology on *CMYC* overexpression. Commitment to an epithelial phenotype is a hallmark of EOC cells. OSE cells *in vitro* and *in vivo* are able to switch among epithelial, mesenchymal, and mesothelial phenotypes. (B) Overexpression of *CMYC* increases colony formation efficiency in both anchorage-independent growth assays and in anchorage-dependent colony formation assays (C). (D) Staining with an anti–annexin V antibody followed by flow cytometry analysis reveals significantly fewer apoptotic cells in IOSE^{CMYC} cultures compared with parental cell lines. (E) Cells were incubated with BrdU, and nuclei were stained with anti-BrdU. In *CMYC*-overexpressing cultures, there were significantly larger proportions of cells in the G_2 phase of the cell cycle compared with IOSE counterparts. In panels B to E, the differences for each phenotypic assay between IOSE and IOSE^{CMYC} cells were statistically significant ($P \leq .05$). Error bars, SEM.

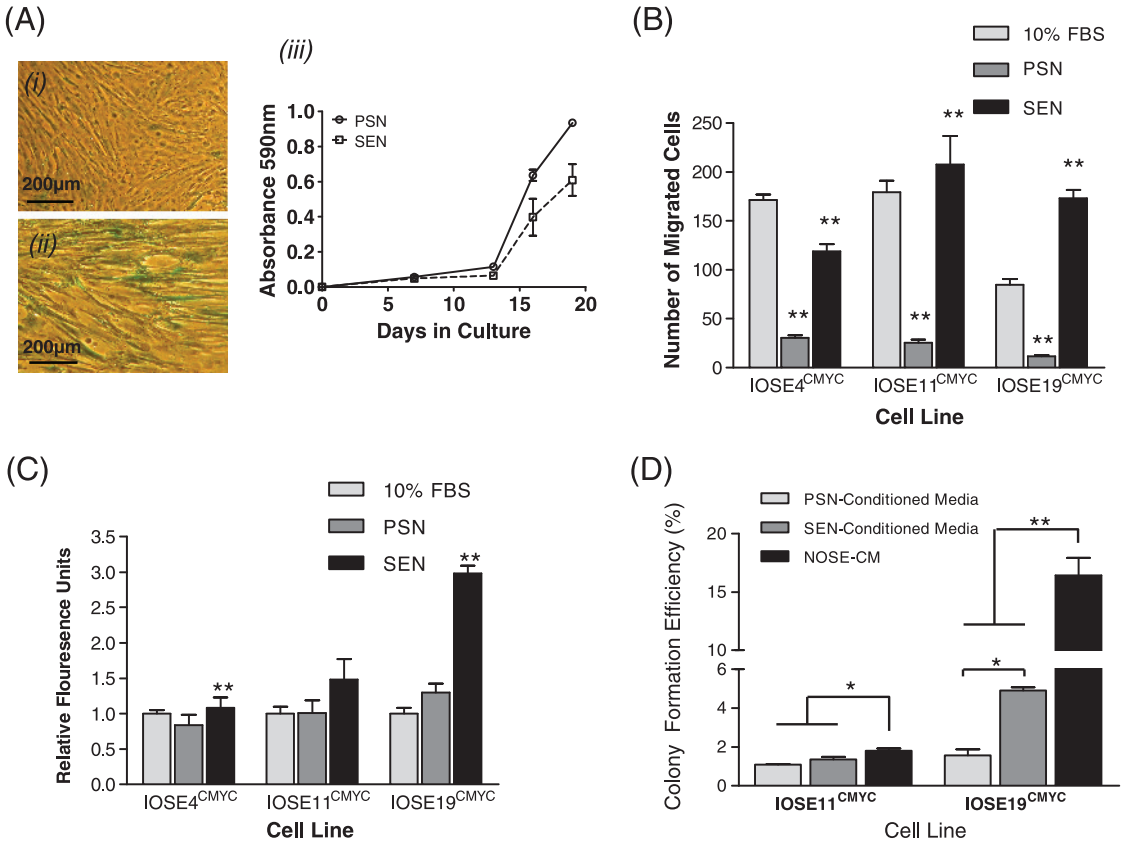

Figure 3. Effects of PSN and SEN fibroblasts on the phenotype of IOSE^{CMYC} cells. (A) Exposing INOFs to hydrogen peroxide (H_2O_2) induces a senescence response that is biologically similar to replicative senescence observed in aging organisms. β-Galactosidase bioactivity confirms senescence induction in INOFs: (*i*) 60% to 80% of SEN stain blue, (*ii*) untreated PSN fibroblasts do not stain, and (*iii*) crystal violet growth assay (absorbance at 595 nm is relative to cell number) show that PSN fibroblasts are more proliferative than SEN fibroblasts. (B) In a migration assay, PSN fibroblasts inhibited motility of IOSE^{CMYC} clones relative to 10% FBS. SEN fibroblasts significantly enhanced migration of all *CMYC* clones relative to a PSN fibroblast chemoattractant. (C) SEN fibroblasts enhanced invasive ability of IOSE^{CMYC} clones relative to PSN fibroblast cells. (D) IOSE19^{CMYC} cells proliferate significantly more in an anchorage-independent growth assay when incubated with conditioned medium from SEN fibroblasts relative to PSN fibroblast conditioned medium. In both SEN/PSN–conditioned media, colony formation efficiency of IOSE^{CMYC} cell lines was reduced relative to standard growth medium (NOSE-CM) (*$P \leq .05$,**$P \leq .01$ by Student's paired *t*-test). Error bars, SEM.

within the ovary create a microenvironment that can trigger neoplastic transformation of dormant, partially transformed ovarian epithelial cells, and that this is a possible explanation for the late-stage development of ovarian cancers from an otherwise inactive organ. In support of this hypothesis, we show for the first time that cellular changes in ovarian stromal fibroblasts can promote neoplastic transformation of OSE cells. This paracrine trigger acts in synergy with early genetic events in partially transformed OSE cells but has little or no effect on untransformed OSE cells.

We modeled the earliest stages of OSE transformation by overexpressing the *CMYC* oncogene in *hTERT*-immortalized OSE cells (IOSE^{CMYC}) because both *hTERT* and *CMYC* are commonly overexpressed in EOCs [29,30]. IOSE^{CMYC} cell lines show evidence of anchorage-independent growth but not invasion, confirming that they are only partially transformed. We observed some variability in the response of different cell lines to *CMYC* overexpression, although the phenotypic trends were the same for all three cell lines; this variation may be the result of subtle differences in the underlying genetic background of the individuals from which the different cell lines were established, influencing the phenotype. When we tested the effects of coculturing IOSE and IOSE^{CMYC} cells with PSN and SEN fibroblasts, we found that SEN fibroblasts had a significant effect on increasing neoplastic transformation of IOSE^{CMYC} cells compared with PSN fibroblasts; neither PSN nor SEN fibroblasts appeared to transform IOSE cells. In anchorage-independent growth assays, we also found that conditioned medium taken from cultured SEN fibroblasts had the ability to promote the neoplastic phenotype of IOSE^{CMYC} cells relative to the conditioned medium harvested from PSN fibroblasts. Taken together, these data suggest that the regulation of neoplastic epithelial cells by PSN/SEN fibroblasts is mediated, at least in part, by soluble, secreted factors.

Key to performing these studies was our ability to generate and characterize an immortalized NOF (INOF) cell line. To our knowledge, this represents the first report detailing the generation of such a line. We were able to confirm the normal, nontransformed, and fibroblastic nature of this cell line, suggesting that it is a relevant model of NOFs. Senescent fibroblasts were also created from the same INOF cell line after exposure to hydrogen peroxide, and so it is unlikely that any of the experimental differences we see between SEN and PSN fibroblasts are the result of differences in the genetic background of cells taken from different individuals.

Inducing senescence-like growth arrest after exposure to hydrogen peroxide has been described previously, and senescent cells have subsequently been shown to exhibit many of the features that are in common with replicative senescence (e.g., β-galactosidase expression, G_1 arrest, enlarged morphology, transcriptomic changes) [12,23,31]. Other mechanisms of inducing cellular senescence can be considered including exposure to bleomycin sulfate, but there is no evidence in the literature to suggest that bleomycin offers an advantage over hydrogen peroxide [12]. The limited life span of primary ovarian fibroblasts meant that their immortalization using *hTERT* was a necessary step, but immortalized cells bypass replicative senescence, hence the need to perform chemically induced senescence. This study therefore has its limitations because it is unclear how closely stress-induced premature senescence *in vitro*, such as that induced by hydrogen peroxide, reflects age-related senescence *in vivo*.

We were able to examine the morphological and biological characteristics of epithelial-fibroblast interactions and to confirm the neoplastic-promoting effects of senescent fibroblasts after creating a three-dimensional heterotypic model of the ovary. This is the first time that a heterotypic three-dimensional model of the normal ovary has been described. In three-dimensional cultures, senescent fibroblasts enhanced proliferation and nuclear atypia in IOSE^{CMYC} cells relative to presenescent and, to a lesser extent, the proliferation of IOSE cell lines.

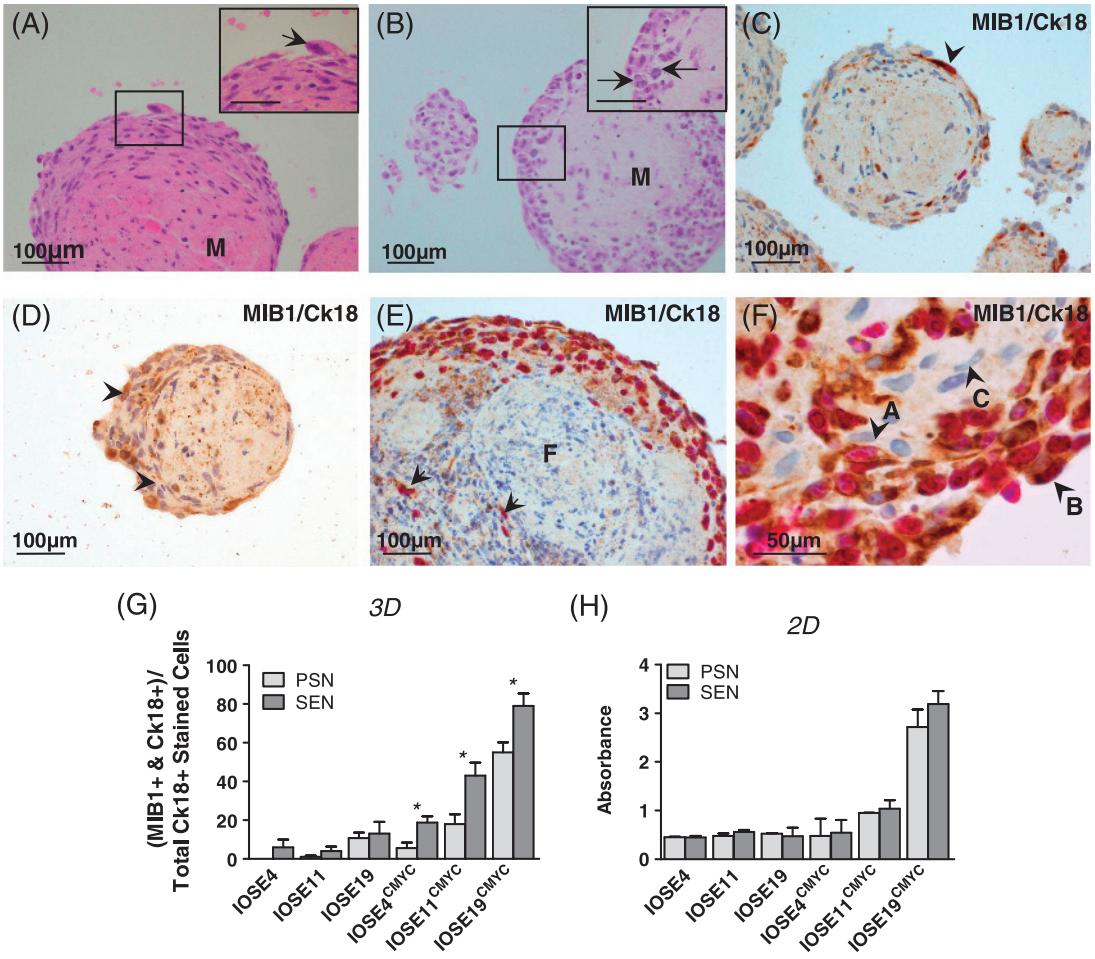

Figure 4. Three-dimensional (3D) *in vitro* modeling of stromal-epithelial interactions. (A) In SEN-IOSE three-dimensional cocultures, "giant" cells (arrow) were observed within peripheral regions of the spheroids. Spheroids contained abundant matrix protein "**M**." (B) In SEN-IOSE^{CMYC} three-dimensional coculture, there was a large peripheral region of plump cells containing some mitotic figures (arrows). (C–F) INOF-IOSE cocultures dual stained for MIB-1 (pink nuclear stain, proliferation marker) and Ck18 (brown cytoplasmic stain). Unstained cells are counterstained with hematoxylin (blue). (C) In SEN-IOSE cocultures, cytokeratin-positive cells are located in the peripheral region of the spheroid (arrowhead). A Ck18$^+$/MIB-1$^+$ dual-positive cell (arrow) is visible in the largest spheroid. (D) In PSN-IOSE cocultures, nonspecific staining of matrix protein can be distinguished by the absence of cellular structure. (E) SEN-IOSE^{CMYC} three-dimensional coculture viewed at low magnification shows the central Ck18-negative staining fibroblastic population "**F**" and peripherally located Ck18-positive stained cells within the spheroid. Some peripheral Ck18-positive stained cells, dual stained for MIB-1 (pink nuclei), can also be seen. (F) In SEN-IOSE^{CMYC} three-dimensional cocultures negative Ck18 stain fibroblasts "**C**" closely interact with the population of Ck18-positive staining epithelial cells "**A**" and "**B**." Note the spindled morphology and elongated nucleus of Ck18-negative cells (e.g., cell **C**) compared with the plump morphology and rounded nuclei of Ck18-positive cells. Cell **A** is positive for Ck18 and negative for MIB-1; cell **B** is positive for both Ck18 and MIB-1. (G) Analysis of dual-stained Ck18/MIB-1–positive cells reveals enhanced proliferation in IOSE^{CMYC} cells when cocultured three-dimensionally with SEN fibroblasts compared with PSN fibroblasts (*$P \leq .05$, Student's paired *t*-test). The proportion of MIB-1 cells is calculated as a ratio of the total Ck18$^+$ population of the culture. (H) Two-dimensional (2D) indirect coculture; crystal violet staining. Epithelial cells do not show significant differences in rates of proliferation when cocultured with SEN or PSN fibroblasts.

This suggests that even the earliest neoplastic changes in normal ovarian epithelia may render cells susceptible to a tumor-promoting trigger from the microenvironment. Our data also suggest that the synergistic relationship between senescent fibroblasts and epithelial cells may continue as tumorigenesis progresses. This is consistent with studies by Yang et al. [32] who have shown that inducing senescence in fibroblasts increases the *in vivo* tumorigenicity of coinjected OSE cells expressing SV40 large-T antigen.

If the results of these studies are real, and the accumulation of metabolically active senescent fibroblasts does act as the microenvironmental trigger for ovarian cancer development, then it raises the question, "what are the secretary factors responsible for epithelial cell transformation?" Some candidates have been identified from previous studies, including osteopontin, stromal cell–derived factor (SDF-1), vascular endothelial growth factor, amphiregulin, hepatocyte growth factor, and interleukin-6, all of which have been shown to act as mediators of the differential paracrine effects of presenescent and senescent fibroblasts [9,11–13,15]. The tumor-promoting effects of the conditioned medium from SEN-IOSE^{CMYC} cocultures compared with the medium from PSN-IOSE^{CMYC} cocultures suggest a possible biological comparison that could be used to identify such factors in the future.

In conclusion, we have used an *in vitro* model of early-stage neoplastic transformation of normal ovarian epithelial cells to test the hypothesis that the accumulation of senescent fibroblasts in aging ovaries can act as a trigger to the rapid development of ovarian cancers—this is consistent with many well-established epidemiological risk factors for ovarian cancer. These effects may be due to the loss of an inhibitory factor, secreted by normal fibroblasts, which inhibits carcinogenesis of epithelial cells harboring mutation(s). Thus, loss of this inhibitory signal on fibroblast senescence may create a microenvironment that is permissive for tumor development. Alternatively, senescent fibroblasts may produce factors that promote transformation of neoplastically transformed epithelia. Support for this hypothesis has come from the analysis of human ovarian tumors, which have been shown to contain a large number of senescent fibroblasts within the tumor stroma; this may also suggest a role for senescent fibroblasts in the maintenance of ovarian tumors [32]. However, testing such a hypothesis *in vivo* in normal ovaries is challenging. There are no reports of the rates of cellular senescence in human ovaries and to study this would probably require mass sectioning and analysis of large numbers of normal ovaries to identify senescent cells. This may be possible using a β-galactosidase bioactivity assay, which enables sensitive detection of senescent cells in frozen tissue specimens. Another way to address the hypothesis, and a focus of future studies, is to evaluate the tumorigenic phenotype of three-dimensional heterotypic models of senescent and presenescent fibroblasts with partially transformed normal ovarian epithelial cells after implantation into immunosuppressed mice.

Acknowledgments

The authors thank the staff at UCLH, the patients who kindly consent to partake in our studies, and John F. Timms for critical review of the manuscript.

References

[1] Yancik R (1993). Ovarian cancer. Age contrasts in incidence, histology, disease stage at diagnosis, and mortality. *Cancer* **71**(2 suppl), 517–523.

[2] Smith ER and Xu XX (2008). Ovarian ageing, follicle depletion, and cancer: a hypothesis for the aetiology of epithelial ovarian cancer involving follicle depletion. *Lancet Oncol* **9**(11), 1108–1111.

[3] Purdie DM, Bain CJ, Siskind V, Webb PM, and Green AC (2003). Ovulation and risk of epithelial ovarian cancer. *Int J Cancer* **104**(2), 228–232.

[4] Pike MC, Pearce CL, Peters R, Cozen W, Wan P, and Wu AH (2004). Hormonal factors and the risk of invasive ovarian cancer: a population-based case-control study. *Fertil Steril* **82**(1), 186–195.

[5] Herbig U, Ferreira M, Condel L, Carey D, and Sedivy JM (2006). Cellular senescence in aging primates. *Science* **311**(5765), 1257.

[6] Jeyapalan JC, Ferreira M, Sedivy JM, and Herbig U (2007). Accumulation of senescent cells in mitotic tissue of aging primates. *Mech Ageing Dev* **128**(1), 36–44.

[7] Olumi AF, Grossfeld GD, Hayward SW, Carroll PR, Tlsty TD, and Cunha GR (1999). Carcinoma-associated fibroblasts direct tumor progression of initiated human prostatic epithelium. *Cancer Res* **59**(19), 5002–5011.

[8] Parrinello S, Coppe JP, Krtolica A, and Campisi J (2005). Stromal-epithelial interactions in aging and cancer: senescent fibroblasts alter epithelial cell differentiation. *J Cell Sci* **118**(Pt 3), 485–496.

[9] Studebaker AW, Storci G, Werbeck JL, Sansone P, Sasser AK, Tavolari S, Huang T, Chan MW, Marini FC, Rosol TJ, et al. (2008). Fibroblasts isolated from common sites of breast cancer metastasis enhance cancer cell growth rates and invasiveness in an interleukin-6–dependent manner. *Cancer Res* **68**(21), 9087–9095.

[10] Krtolica A, Parrinello S, Lockett S, Desprez PY, and Campisi J (2001). Senescent fibroblasts promote epithelial cell growth and tumorigenesis: a link between cancer and aging. *Proc Natl Acad Sci USA* **98**(21), 12072–12077.

[11] Begley L, Monteleon C, Shah RB, Macdonald JW, and Macoska JA (2005). CXCL12 overexpression and secretion by aging fibroblasts enhance human prostate epithelial proliferation *in vitro*. *Aging Cell* **4**(6), 291–298.

[12] Bavik C, Coleman I, Dean JP, Knudsen B, Plymate S, and Nelson PS (2006). The gene expression program of prostate fibroblast senescence modulates neoplastic epithelial cell proliferation through paracrine mechanisms. *Cancer Res* **66**(2), 794–802.

[13] Pazolli E, Luo X, Brehm S, Carbery K, Chung JJ, Prior JL, Doherty J, Demehri S, Salavaggione L, Piwnica-Worms D, et al. (2009). Senescent stromal-derived osteopontin promotes preneoplastic cell growth. *Cancer Res* **69**(3), 1230–1239.

[14] Coppé JP, Patil CK, Rodier F, Sun Y, Muñoz DP, Goldstein J, Nelson PS, Desprez PY, and Campisi J (2008). Senescence-associated secretory phenotypes reveal cell-nonautonomous functions of oncogenic RAS and the p53 tumor suppressor. *PLoS Biol* **6**(12), 2853–2868.

[15] Coppé JP, Kauser K, Campisi J, and Beauséjour CM (2006). Secretion of vascular endothelial growth factor by primary human fibroblasts at senescence. *J Biol Chem* **281**(40), 29568–29574.

[16] Liu D and Hornsby PJ (2007). Senescent human fibroblasts increase the early growth of xenograft tumors via matrix metalloproteinase secretion. *Cancer Res* **67**(7), 3117–3126.

[17] Lawrenson K, Benjamin E, Turmaine M, Jacobs IJ, Gayther SA, and Dafou D (2009). *In vitro* three-dimensional modelling of human ovarian surface epithelial cells. *Cell Prolif* **42**(3), 385–393.

[18] Dimri GP, Lee X, Basile G, Acosta M, Scott G, Roskelley C, Medrano EE, Linskens M, Rubelj I, Pereira-Smith O, et al. (1995). A biomarker that identifies senescent human cells in culture and in aging skin *in vivo*. *Proc Natl Acad Sci USA* **92**(20), 9363–9367.

[19] Iyer VR, Eisen MB, Ross DT, Schuler G, Moore T, Lee JC, Trent JM, Staudt LM, Hudson J Jr, Boguski MS, et al. (1999). The transcriptional program in the response of human fibroblasts to serum. *Science* **283**, 83–87.

[20] Chang HY, Sneddon JB, Alizadeh AA, Sood R, West RB, Montgomery K, Chi JT, van de Rijn M, Botstein D, and Brown PO (2004). Gene expression signature of fibroblast serum response predicts human cancer progression: similarities between tumors and wounds. *PLoS Biol* **2**(2), e7.

[21] Herbert BS, Wright WE, and Shay JW (2002). p16(INK4a) inactivation is not required to immortalize human mammary epithelial cells. *Oncogene* **21**(51), 7897–7900.

[22] Darbro BW, Lee KM, Nguyen NK, Domann FE, and Klingelhutz AJ (2006). Methylation of the p16(INK4a) promoter region in telomerase immortalized human keratinocytes co-cultured with feeder cells. *Oncogene* **25**(56), 7421–7433.

[23] Milyavsky M, Shats I, Erez N, Tang X, Senderovich S, Meerson A, Tabach Y, Goldfinger N, Ginsberg D, Harris CC, et al. (2003). Prolonged culture of

telomerase-immortalized human fibroblasts leads to a premalignant phenotype. *Cancer Res* **63**(21), 7147–7157.

[24] Li NF, Broad S, Lu YJ, Yang JS, Watson R, Hagemann T, Wilbanks G, Jacobs I, Balkwill F, Dafou D, et al. (2007). Human ovarian surface epithelial cells immortalized with hTERT maintain functional pRb and p53 expression. *Cell Prolif* **40**(5), 780–794.

[25] Shao G, Balajee AS, Hei TK, and Zhao Y (2008). $p16^{INK4a}$ downregulation is involved in immortalization of primary human prostate epithelial cells induced by telomerase. *Mol Carcinog* **47**(10), 775–783.

[26] Fathalla MF (1971). Incessant ovulation—a factor in ovarian neoplasia? *Lancet* **2**(7716), 163.

[27] Couzinet B, Meduri G, Lecce MG, Young J, Brailly S, Loosfelt H, Milgrom E, and Schaison G (2001). The postmenopausal ovary is not a major androgen-producing gland. *J Clin Endocrinol Metab* **86**(10), 5060–5066.

[28] Cai KQ, Klein-Szanto A, Karthik D, Edelson M, Daly MB, Ozols RF, Lynch HT, Godwin AK, and Xu XX (2006). Age-dependent morphological alterations of human ovaries from populations with and without *BRCA* mutations. *Gynecol Oncol* **103**(2), 719–728.

[29] Brustmann H (2005). Immunohistochemical detection of human telomerase reverse transcriptase (*hTERT*) and c-kit in serous ovarian carcinoma: a clinicopathologic study. *Gynecol Oncol* **98**(3), 396–402.

[30] Dimova I, Raitcheva S, Dimitrov R, Doganov N, and Toncheva D (2006). Correlations between c-*myc* gene copy-number and clinicopathological parameters of ovarian tumours. *Eur J Cancer* **42**(5), 674–679.

[31] Bladier C, Wolvetang EJ, Hutchinson P, de Haan JB, and Kola I (1997). Response of a primary human fibroblast cell line to H_2O_2: senescence-like growth arrest or apoptosis? *Cell Growth Differ* **8**(5), 589–598.

[32] Yang G, Rosen DG, Zhang Z, Bast RC Jr, Mills GB, Colacino JA, Mercado-Uribe I, and Liu J (2006). The chemokine growth–regulated oncogene 1 (*Gro-1*) links RAS signaling to the senescence of stromal fibroblasts and ovarian tumorigenesis. *Proc Natl Acad Sci USA* **103**(44), 16472–16477.

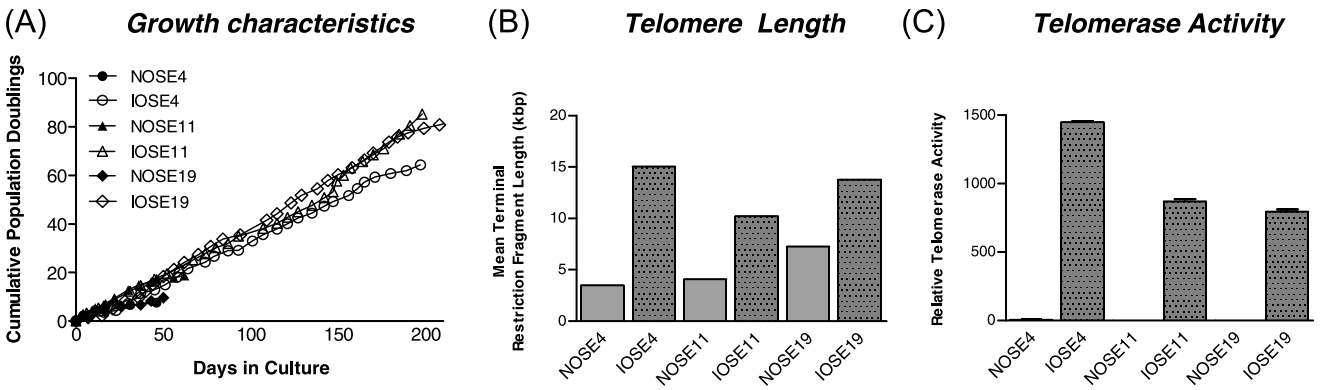

(D)

CELL LINE	ANTIBODY						
	Ck7	BerEP4	CA125	E-Cadherin	AE1/AE3	FSP	Calretinin
NOSE4	++	++	+/-	-	+	-	+
IOSE4	+++	+	+/-	-	++	-	+/-
NOSE11	+++	++	+	-	++	+/-	++
IOSE11	++	+	-	-	++	-	+
NOSE19	++	-	+	-	++	+/-	+
IOSE19	+++	+	-	-	+/-	-	+/-

+++ 70-100% cells stain positive
++ 40-70% cells stain positive
+ 10-40% cells stain positive
+/- Under 10% cells stain positive
- No cells stain positive

Figure W1. Immortalization of primary NOSE cells. The three IOSE cell lines have been maintained in culture for more than 200 days without signs of transformation: the cells do not grow in anchorage-independent growth assays and do not stain for CA-125 or E-cadherin, which is commonly expressed in ovarian epithelial tumors. (A) *In vitro* life span of primary NOSE cells is typically around 50 days. Immortalized OSE (IOSE) cells have been passaged for more than 200 days to date. Primary cells were immortalized by the ectopic expression of *hTERT*. (B) Telomere terminal restriction fragment length is increased in IOSE cell lines compared with parental NOSE cultures. (C) Telomerase activity, detected by PCR-ELISA, is absent in primary cultures but present in immortalized cell lines. (D) Staining for cytokeratin (Ck7), BerEP4, CA-125, E-cadherin, pan-cytokeratin (AE1/AE3), FSP, and calretinin by fluorescent immunocytochemistry reveals that primary NOSE and IOSE have similar staining profiles.